# Activity-induced tissue oxygenation changes in rat cerebellar cortex: interplay of postsynaptic activation and blood flow

Nikolas Offenhauser[1], Kirsten Thomsen[1], Kirsten Caesar[1] and Martin Lauritzen[1,2]

[1]*Department of Medical Physiology, The Panum Institute, University of Copenhagen, Blegdamsvej 3, 2200 Copenhagen N, Denmark*
[2]*Department of Clinical Neurophysiology, Glostrup Hospital, 2600 Glostrup, Denmark*

**Functional neuroimaging relies on the robust coupling between neuronal activity, metabolism and cerebral blood flow (CBF), but the physiological basis of the neuroimaging signals is still poorly understood. We examined the mechanisms of activity-dependent changes in tissue oxygenation in relation to variations in CBF responses and postsynaptic activity in rat cerebellar cortex. To increase synaptic activity we stimulated the monosynaptic, glutamatergic climbing fibres that excite Purkinje cells via AMPA receptors. We used local field potentials to indicate synaptic activity, and recorded tissue oxygen partial pressure ($P_{\mathrm{tiss,O_2}}$) by polarographic microelectrodes, and CBF using laser-Doppler flowmetry. The disappearance rate of oxygen in the tissue increased linearly with synaptic activity. This indicated that, without a threshold, oxygen consumption increased as a linear function of synaptic activity. The reduction in $P_{\mathrm{tiss,O_2}}$ preceded the rise in CBF. The time integral (area) of the negative $P_{\mathrm{tiss,O_2}}$ response increased non-linearly showing saturation at high levels of synaptic activity, concomitant with a steep rise in CBF. This was accompanied by a positive change in $P_{\mathrm{tiss,O_2}}$. Neuronal nitric oxide synthase inhibition enhanced the initial negative $P_{\mathrm{tiss,O_2}}$ response ('dip'), while attenuating the evoked CBF increase and positive $P_{\mathrm{tiss,O_2}}$ response equally. This indicates that increases in CBF counteract activity-induced reductions in $P_{\mathrm{tiss,O_2}}$, and suggests the presence of a tissue oxygen reserve. The changes in $P_{\mathrm{tiss,O_2}}$ and CBF were strongly attenuated by AMPA receptor blockade. Our findings suggest an inverse relationship between negative $P_{\mathrm{tiss,O_2}}$ and CBF responses, and provide direct *in vivo* evidence for a tight coupling between activity in postsynaptic AMPA receptors and cerebellar oxygen consumption.**

(Received 6 January 2005; accepted after revision 14 March 2005; first published online 17 March 2005)
**Corresponding author** N. Offenhauser: University of Copenhagen, Department of Medical Physiology, The Panum Institute 12.5, Blegdamsvej 3, DK-2200 Copenhagen N, Denmark. Email: nikolas@offenhauser.de

Nerve tissue is among the highest oxygen-consuming tissues in the body. The oxygen is used for oxidation of glucose which is thought to provide almost all the energy needed by neurones to support brain activity (Siesjo, 1978). There is a tight coupling between neuronal activity, blood flow and glucose and oxygen consumption (Clarke & Sokoloff, 1994). The tight and robust neurovascular coupling (Iadecola, 2004) is driven by synaptic mechanisms (Lauritzen, 2005), and ensures that oxygen and glucose are supplied to the brain to match activity (Raichle, 1998). There is a strong interest in exploring the energetic costs of single elements of chemical neurotransmission in order to provide an energy budget for signalling in the grey matter of the brain (Attwell & Laughlin, 2001; Lennie, 2003). This, as well as an exact knowledge of the timing and the quantitative relationship between neuronal activities, blood flow and oxygen consumption, forms the basis for correct interpretation of signals obtained by functional neuroimaging in the working brain (Raichle, 2003; Obata *et al.* 2004).

The aim of the present work was to investigate oxygen consumption by examining the changes in tissue oxygen partial pressure ($P_{\mathrm{tiss,O_2}}$) during activation in a simple neuronal network in relation to excitatory synaptic activity and changes in blood flow. We chose the excitatory, monosynaptic glutamatergic climbing fibre–Purkinje cell synapse for that purpose. One of the advantages of this system is that synaptic excitation is robust, and that the cerebral blood flow (CBF) response develops slowly during stimulation; that is, over tens of seconds (Mathiesen *et al.* 1998). In comparison, the CBF response in the somatosensory system develops much faster; that is,

 DOI: 10.1113/jphysiol.2005.082776

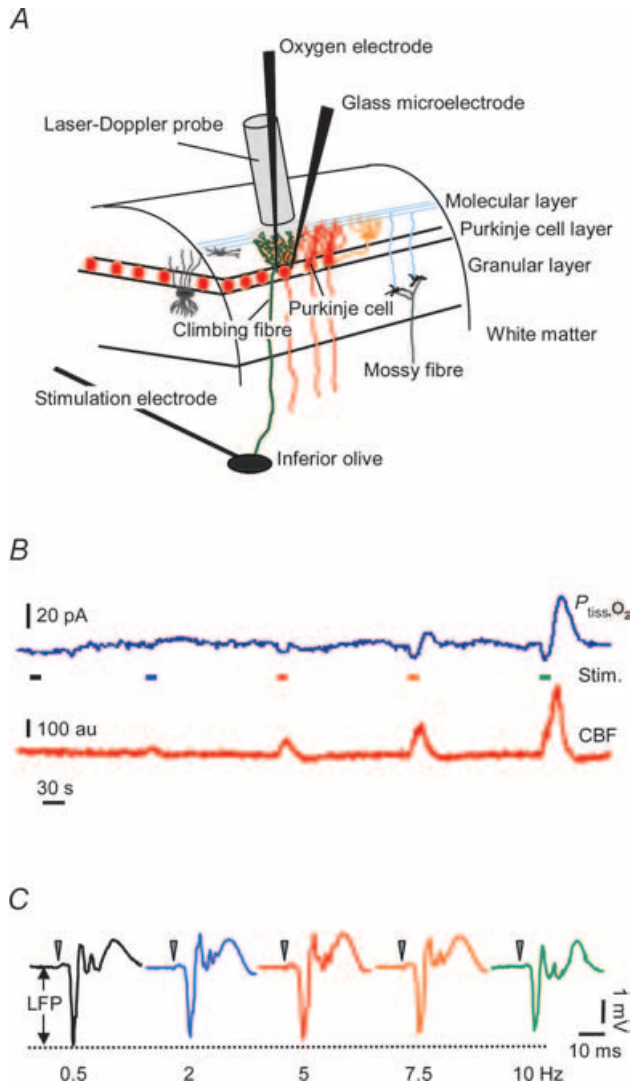


**Figure 1. Recordings of $P_{tiss,O_2}$, neuronal activity and blood flow in rat cerebellar cortex**
*A*, schematic three-dimensional drawing of experimental set-up, including neurones of interest and placement of stimulation and recording devices. A bi-polar electrode placed stereotaxically in the caudal part of the inferior olive stimulated climbing fibres (green) that give a monosynaptic excitatory input to Purkinje cells (red). Concurrent electrophysiological recordings (LFPs) were performed by a glass microelectrode at the level of the Purkinje cell layer. An oxygen microelectrode located at the same depth, simultaneously recorded changes in tissue oxygen tension ($P_{tiss,O_2}$). A specific characteristic of this modified Clark-type polarographic electrode is its built-in guard cathode, which promotes the long-term stability of oxygen measurements. Tip diameter ranged from 3 to 5 $\mu$m. CBF was recorded by LDF with a probe located in close apposition to the microelectrodes. *B*, shows original recordings of both $P_{tiss,O_2}$ (upper trace) and CBF (lower trace) in response to climbing fibre stimulation with increasing stimulation frequency. Coloured bars indicate stimulation periods (15 s) and frequencies (same colour code as in *C*). *C*, the corresponding averaged LFPs for each stimulation frequency, where LFP amplitudes tended to decrease with increasing frequencies. The double-headed arrow indicates the measured LFP amplitude for the 0.5-Hz stimulation. Time points of stimulation are marked by grey arrowheads. Examples are from the same animal as in Fig. 2.

of the order of hundreds of milliseconds (Nielsen & Lauritzen, 2001), which may cloud rapid initial decreases in $P_{tiss,O_2}$. Therefore, the chances of observing changes in $P_{tiss,O_2}$ independently of blood flow changes were greater in the cerebellar cortex. This allowed us to explore the basis for the activity-induced initial 'dip', and the following overshoot in tissue oxygenation. As far as we can ascertain, this is the first study to simultaneously measure tissue oxygenation changes and CBF responses to a wide range of synaptic activation and quantitatively assess their relationships. Specifically, we tested the hypothesis that clamping the CBF response by inhibiting activity-dependent vasodilatation would enhance the oxygen dip without affecting the evoked synaptic activity. At the same time we examined the hypothesis that the tissue oxygenation overshoot that follows the initial early oxygen dip depended on the rise in blood flow. Finally, we tested the hypothesis that blocking postsynaptic activity by glutamatergic AMPA receptor inhibitors would block the early oxygen dip.

## Methods

### Animal preparation

Experiments were performed in 26 male Wistar rats (250–350 g). The study was in full compliance with the guidelines of the European Council's Convention for the Protection of Vertebrate Animals Used for Experimental and Other Scientific Purposes and was approved by the Danish National Ethics Committee. Anaesthesia was induced with isoflurane (5.0% for induction, 1.5% during surgery). After surgery, anaesthesia was switched to intravenous $\alpha$-chloralose (bolus, 45 mg kg$^{-1}$; supplement, 15 mg kg$^{-1}$ (20 min)$^{-1}$) for at least 1 h before data acquisition. Extra supplements of $\alpha$-chloralose were given upon pilo-erection or increased blood pressure (> 10%). The trachea was cannulated for mechanical ventilation (30% $O_2$–70% $N_2O$ during surgery; $O_2$-enriched air thereafter) and the left femoral vein and artery for anaesthesia delivery and for continuous monitoring of mean arterial blood pressure (MABP) and periodic arterial blood gas sampling, respectively (MABP, 108 ± 1 mmHg; $P_{CO_2}$, 36.8 ± 0.3 mmHg; $P_{O_2}$, 123.9 ± 2.0 mmHg; pH 7.39 ± 0.004; mean ± S.E.M.; $n = 26$). Rectal temperature was monitored and maintained at 37 ± 0.5°C. Intraperitoneal catheters were inserted for application of 7-nitroindazole (7-NI). The animals were placed in a head holder with lignocaine (lidocaine) gel (2%) applied to the contact spots of the ear bars. An open cranial window preparation was placed over parts of the cerebellar vermis and medulla oblongata, and the brain was superfused with artificial cerebrospinal fluid (aCSF) as previously described (Mathiesen *et al.* 1998). At the end of the experiment animals were killed by an intravenous injection of air. The experimental setup is depicted in Fig. 1.

### Electrophysiological recordings

A single-barrelled glass microelectrode filled with 2 M saline (impedance, 2–3 MΩ; tip diameter, ∼2 μm) was lowered to a depth of 300–500 μm into the vermis of the cerebellar cortex. An Ag–AgCl ground electrode was placed in the neck muscle. Extracellular local field potentials (LFPs) and single unit activity (spikes) of Purkinje cells were recorded at the level of the Purkinje cell layer. Purkinje cells were identified by their ability to fire both simple and complex spikes spontaneously or the production of a complex spike at 5–8 ms after electrical stimulation of the inferior olive. The preamplified (× 10) signal was A/D-converted, amplified, filtered (spikes, 300–6000 Hz bandwidth; LFPs, 0.5–2400 Hz bandwidth) and digitally sampled using the Power 1401 interface (Cambridge Electronic Design, Cambridge, UK) connected to a PC running the Spike 2.5 software (Cambridge Electronic Design). Digital sampling rates were at 25 kHz for spikes and 5 kHz for LFPs.

### Climbing fibre stimulation

A coated, bipolar stainless steel electrode (SNEX 200, Rhodes Medical Instruments, Inc., Woodland Hills, CA, USA; contact separation, 0.25 mm) was stereotaxically lowered into the caudal part of the inferior olive as described (Mathiesen *et al.* 1998). Positioning was optimized by means of the maximal response of LFPs to low-frequency stimulation (0.5 Hz) and by the occurrence of complex spikes in response to stimulation. Each Purkinje cell receives excitatory input from one climbing fibre that makes synaptic contact with the Purkinje cell soma and proximal dendrites. Climbing fibre stimulation induces release of glutamate, which activates Purkinje cells via postsynaptic AMPA receptors (Mathiesen *et al.* 1998), resulting in activation of Purkinje cells located within parasagittal bands (Dunbar *et al.* 2004). In optical imaging studies and multiple electrode recordings the width of these bands in the mediolateral direction ranged from 250 to 500 μm (Hanson *et al.* 2000; Fukuda *et al.* 2001). Stimulation was given as 0.2-ms square-wave pulses at 0.15 mA (ISO-flex, A.M.P.I., Israel) with increasing frequencies for 15 s. We used stimulation frequencies between 0.5 and 10 Hz; 10 Hz corresponds to the highest firing frequency of the inferior olive–climbing fibre system (Llinas & Volkind, 1973; Llinas *et al.* 2002) and evoked synaptic currents might be unreliable above this frequency (Silver *et al.* 1998).

### Protocol

Three sets of experiments were performed for this study. First, we examined the relationship between increases in excitatory synaptic activity and local changes in $P_{\mathrm{tiss,O_2}}$ and CBF within the activated region. To increase neuronal activity we stimulated climbing fibres with increasing frequencies of 0.5, 2, 5, 7.5 and 10 Hz ($n = 10$). We correlated the summed LFP (ΣLFP, see below) to evoked changes in $P_{\mathrm{tiss,O_2}}$ and CBF to obtain a quantitative relationship between these variables.

In the second part of the study, we clamped CBF during activation thereby diminishing the supply of $O_2$ to the activated area. To this end, we applied the neuronal nitric oxide synthase (nNOS, type I NOS) inhibitor, 7-NI (40 mg kg$^{-1}$ I.P., in 5% cremophor; Sigma Chemicals, Vallensbaek, Denmark; $n = 8$). Climbing fibres were stimulated at 10 Hz and the responses compared before (CTR) and 30 min after drug application (7-NI).

Finally, we wanted to establish whether postsynaptic activity in Purkinje cells could explain the oxygen consumption found during activation. Thus, the third part of this study examined the effect of AMPA receptor blockade on activation-induced $P_{\mathrm{tiss,O_2}}$ changes. We superfused the cerebellum with the AMPA receptor antagonist 6-cyano-7-nitroquinoxaline-2,3-dione (CNQX; 0.5 mM in aCSF; $n = 8$). Responses to stimulation at 10 Hz were compared before (CTR), during CNQX (CNQX), and after a wash out period (Wash out). Additionally, in five of the 7-NI-treated animals from the second part of the study, CNQX (0.5 mM) was applied after 7-NI had been given. In order to obtain complete recovery of responses, CNQX application was kept brief and no attempt was made to achieve a complete attenuation of signals in all animals. Only animals exhibiting a significant negative $P_{\mathrm{tiss,O_2}}$ response (area below 2 S.D. from baseline) were included in the CNQX experiments. Interstimulus interval in all three groups was 3 min.

### Cerebellar cortical blood flow measurement

CBF was recorded continuously using laser-Doppler flowmetry (LDF). The LDF probe was at a fixed position ∼0.3 mm above the pial surface in a region devoid of large vessels (wavelengths, 780 nm; fibre separation, 250 μm; PeriMed, Järfälla, Sweden). The probe, measuring CBF changes down to a depth of 1000 μm, was placed as close as possible to the micro- and oxygen electrode. The LDF signal was smoothed with a time constant of 0.2 s (PeriFlux 4001 Master, PeriMed), sampled with 10 Hz, A/D converted and digitally recorded using Spike 2.5 software (Cambridge Electronic Design).

### Tissue $P_{O_2}$ measurements

We used a modified Clark-type polarographic oxygen microelectrode (OX-10, Unisense A/S, Aarhus, Denmark) with a guard cathode for $P_{\mathrm{tiss,O_2}}$ measurements (Revsbech, 1989). The advantage of this electrode type is its small tip size (3–5 μm in this study) and its built-in guard cathode which removes all oxygen from the electrolyte reservoir.

This enabled us to measure $P_{\mathrm{tiss,O_2}}$ over time (and different treatment conditions) with excellent long-term stability (signal drift, 0–0.5% $\mathrm{h^{-1}}$). The field of sensitivity is a sphere of 2 × tip diameter. The electrodes used in this study were constructed so that the 90% response time was < 1 s and the stirring sensitivity was nearly negligible at < 0.8% (Revsbech, 1989). Oxygen microsensors respond linearly to changes in oxygen concentration. Calibration of each electrode was performed in air-saturated and oxygen-free saline (0.9% at 37°C) before and after each experiment with reproducible oxygen measurements. Mean $P_{\mathrm{tiss,O_2}}$ was 38.4 ± 2.6 mmHg (mean ± S.E.M.; $n = 26$) and ranged from 12.7 to 64.4 mmHg. The oxygen electrodes were stepwise, vertically inserted in the cerebellar cortex and positioned in the same sagittal line and at the same cortical depth as the glass microelectrodes. The distance between the two electrodes was ∼100–200 $\mu$m. Both electrodes and the LDF probe recorded from the same cerebellar folia and were kept in the same position throughout the experiment. No linear drifts in baseline occurred during the experiments. The oxygen electrodes were connected to a high impedance picoammeter (PA 2000, Unisense A/S) sensing the currents of the oxygen electrodes. Signals were A/D converted and recorded at 100 Hz (Power 1401 and Spike 2.5 (Cambridge Electronic Design)). Off-line filtering using a low-pass filter of 0.3 Hz was used to remove noise induced by heartbeat and mechanical ventilation as described by Masamoto *et al.* (2003*a*).

### Data analysis and statistics

Simultaneously recorded LFP, CBF and $P_{\mathrm{tiss,O_2}}$ signals were used for analysis. Stimulation-induced CBF and $P_{\mathrm{tiss,O_2}}$ responses were calculated as percentage change from baseline (20 s prior to stimulation). The magnitude of the response was estimated as the area under the curve above (CBF, positive $P_{\mathrm{tiss,O_2}}$ responses) or below (negative $P_{\mathrm{tiss,O_2}}$ responses) two standard deviations of baseline. This, in conjunction with the long baseline period, ensured that only statistically significant responses were included for further analysis. Individual animals had constant levels of baseline noise throughout the experiment. The initial slope (disappearance rate of oxygen in the tissue; $-k$) of the early $P_{\mathrm{tiss,O_2}}$ decrease is useful as an indicator of local oxygen consumption (Leniger-Follert, 1977). $-k$ was calculated from the initial constant decrease phase of the negative $P_{\mathrm{tiss,O_2}}$ response (∼1–3 s after stimulation onset). $-k$ was determined as the tangent of the steeply decreasing $P_{\mathrm{tiss,O_2}}$ curve during this period and is defined as the difference in tissue oxygen partial pressure (in percentage change from baseline) divided by time (in seconds). The initial slope was not calculated for the CNQX-treatment group because negative $P_{\mathrm{tiss,O_2}}$ responses were abolished or too small during CNQX application to obtain reliable initial slope calculations. Calculating oxygen consumption from the initial slope requires the determination of oxygen release from haemoglobin in the area of interest. Due to this, and the well-described spatial heterogeneity of brain $P_{\mathrm{tiss,O_2}}$ and local oxygen consumption (Leniger-Follert, 1977; Erecinska & Silver, 2001; Baumgartl *et al.* 2002; Masamoto *et al.* 2003*b*), no attempt was made to calculate local cerebral metabolic rate of oxygen ($\mathrm{CMRO_2}$) in absolute terms from our data. Another practical consequence of this spatial heterogeneity was that the temporal profiles of $P_{\mathrm{tiss,O_2}}$ responses were not averaged for groups of animals. The response magnitudes and the initial slopes of the oxygen signals were calculated for each animal from averaged responses of four to six stimulations per treatment condition or stimulation frequency. Calculations were performed by a custom-made analysis program based on Matlab 6.5 (MathWorks Inc., Natick, MA, USA). Responses in which the oxygen signal did not return to baseline (± 2 S.D.) within 75 s after stimulation onset were excluded.

The LFP is a potential change in the extracellular fluid induced by ion fluxes resulting from synchronized activity of ensembles of nerve cells (Llinas & Nicholson, 1974). LFPs in the cerebellar cortex are characterized by dendritic transmembrane ion fluxes (Nicholson & Llinas, 1971). Climbing fibre stimulation-induced LFPs consist of a negligible presynaptic component and a large excitatory postsynaptic potential which is followed by a smaller and slower positive potential (Eccles *et al.* 1967). A net influx of positive ions into the dendrites of Purkinje cells at the site of synaptic excitation produces a current sink and causes the negative deflection of the LFP. The following decline in negative potential and even its reversal to a positive wave are attributable to the somata and axons of the Purkinje cells, where a net efflux of positive ions acts as a current source (Eccles *et al.* 1966). We calculated LFP amplitudes as the difference between the large negative deflection and the baseline before stimulation onset. Additional off-line digital low-pass filtering (0.5–300 Hz) of the LFP signal ensured that no high frequency (spike) signals contaminated the LFP measurements. Mean LFP amplitudes were calculated for each frequency (0.5–10 Hz) or treatment condition (e.g. CTR, 7-NI, CNQX, Wash out) and the summed potential ($\Sigma$LFP) was calculated as the product of the LFP amplitude (in mV) and the stimulus rate (in Hz). The $\Sigma$LFP was used as an indicator of synaptic activity (Mathiesen *et al.* 1998).

To be able to compare data between animals, responses (LFP, CBF, $P_{\mathrm{tiss,O_2}}$) were normalized to the response evoked by 10 Hz stimulation. $\Sigma$LFP was correlated to the evoked CBF and $P_{\mathrm{tiss,O_2}}$ responses, either by least-squares linear regression analysis or by polynomial regression in cases where non-linearity was evident from the distribution of data. All data are expressed as means ± S.E.M. ANOVA on repeated measures followed by Bonferroni *post hoc*

analysis was performed for statistical comparison of multiple treatment conditions. When appropriate for simple comparisons within groups ('before-after'), a paired *t* test was used. Values were considered statistically significant at $P < 0.05$.

## Results

Co-localized synaptic activity, $P_{\mathrm{tiss,O_2}}$ and CBF were simultaneously measured (Fig. 1). We used local field potential recordings, a Clark-type polarographic oxygen microelectrode and a LDF probe to assess the inter-dependency of synaptic activity, $P_{\mathrm{tiss,O_2}}$ and CBF responses and to clarify the nature of the biphasic $P_{\mathrm{tiss,O_2}}$ signals evoked by neuronal activation.

Experiments were performed in the cerebellar cortex using the well-described purely excitatory monosynaptic climbing fibre–Purkinje cell pathway. Stimulation of climbing fibres results in an all-or-none activation of post-synaptic Purkinje cells (Eccles *et al.* 1966). Synaptic transmission in the climbing fibre–Purkinje cell pathway is glutamatergic and results in activation of postsynaptic AMPA receptors (Mathiesen *et al.* 1998; Beitz & Saxon, 2004). Thus, there is a clear association between climbing fibre stimulation and postsynaptic excitatory activity in Purkinje cells (Eccles *et al.* 1966; Llano *et al.* 1991; Konnerth *et al.* 1990; Mathiesen *et al.* 1998) (Fig. 1*C*).

### Frequency-dependent changes in $P_{\mathrm{tiss,O_2}}$ and CBF

We varied the input function by increasing the frequency of climbing fibre stimulation. Evoked responses of local $P_{\mathrm{tiss,O_2}}$ and CBF were frequency-dependent, as illustrated in Figs 1*B*, 2 and 3. The CBF responses were monophasic increments, whereas the $P_{\mathrm{tiss,O_2}}$ response pattern ranged from decreases alone at low frequencies to biphasic responses at higher stimulus frequencies (Fig. 2*A*). The biphasic responses consisted of an initial decrease in $P_{\mathrm{tiss,O_2}}$ (negative $P_{\mathrm{tiss,O_2}}$ response) followed by a slower and longer lasting positive peak (positive $P_{\mathrm{tiss,O_2}}$ response). Comparison of the time courses of the $P_{\mathrm{tiss,O_2}}$ and CBF signals showed that the decrease in $P_{\mathrm{tiss,O_2}}$ began before the increase in CBF was evident (Fig. 2*A*).

The disappearance rate of oxygen in the tissue ($-k$), reflecting early local oxygen consumption during activation, increased as a function of stimulation frequency, which is shown by the increasing initial slope of the negative $P_{\mathrm{tiss,O_2}}$ signal during the first seconds of stimulation (Fig. 2*A* inset, and Fig. 3*A*). In comparison, the magnitude of the area of the negative $P_{\mathrm{tiss,O_2}}$ response increased only up to stimulation frequencies of 5 Hz, after which it clearly levelled off or even decreased (Fig. 3*B*). The area of the positive $P_{\mathrm{tiss,O_2}}$ response paralleled the CBF increase at stimulation frequencies above 5 Hz (Fig. 3*C* and *D*).

### Relationship of ΣLFP to $P_{\mathrm{tiss,O_2}}$ and CBF responses

As a measure of neuronal activation, synaptic activity was calculated for each stimulation train as the average field potential amplitude multiplied by stimulus frequency (ΣLFP). The LFP represents the spatially weighted sum of extracellular currents due to synchronous synaptic activity in a group of neurones in response to one stimulation impulse (Llinas & Nicholson, 1974). The summation of LFP amplitudes over time is therefore a plausible indicator of total synaptic activity evoked by repeated stimulation impulses and has been widely used to describe the inter-relationship of synaptic activity and CBF or metabolism (Mathiesen *et al.* 1998; Devor *et al.* 2003; Sheth *et al.* 2004; Thomsen *et al.* 2004). LFP amplitudes decreased at higher stimulation frequencies (Fig. 1*C*) due to reduced glutamate release (Silver *et al.* 1998; Foster & Regehr, 2004) or postsynaptic AMPA receptor saturation (Harrison & Jahr, 2003). In consequence, ΣLFP started to plateau at frequencies above 5 Hz (Fig. 3*E*).

The relationship between ΣLFP and the initial slope of the negative $P_{\mathrm{tiss,O_2}}$ response ($-k$) is shown in Fig. 2*B* (one animal) and Fig. 4*A* (all animals, normalized data). Evoked synaptic activity was found to be linearly related to $-k$ and the data were well described by a linear regression passing through the origin ($R^2 = 0.987$; $P = 3.37 \times 10^{-6}$). This finding implies that during the early phase of activation, oxygen is consumed at all levels of synaptic activity.

The area of the negative $P_{\mathrm{tiss,O_2}}$ response was calculated to obtain a measure of the integrated effect of synaptic activity on $P_{\mathrm{tiss,O_2}}$ over time. However, in contrast to $-k$, the relationship between the area of the negative $P_{\mathrm{tiss,O_2}}$ response and synaptic activity (ΣLFP) was non-linear (Fig. 4*B*). The negative $P_{\mathrm{tiss,O_2}}$ area increased linearly at low or moderate levels of synaptic activity, but reached a plateau at higher levels. In comparison, neither the area of the positive $P_{\mathrm{tiss,O_2}}$ response nor the CBF response showed signs of saturation with increasing synaptic activity (Fig. 4*C* and *D*). The graphs in Fig. 4*C* and *D* show a non-linear relationship between synaptic activity and CBF, and positive $P_{\mathrm{tiss,O_2}}$ responses, respectively. They also illustrate that the positive $P_{\mathrm{tiss,O_2}}$ response followed the increase in CBF only at higher levels of synaptic activity.

The pattern of these responses suggested strong interaction between the evoked CBF responses and the magnitudes of the negative and positive $P_{\mathrm{tiss,O_2}}$ responses. The negative $P_{\mathrm{tiss,O_2}}$ response area increased as a function of ΣLFP up to the level of synaptic activity at which the magnitude of the CBF response increased sharply. At this point also, the positive $P_{\mathrm{tiss,O_2}}$ response appeared (Fig. 4*B*–*D*). We hypothesized that the activity-induced, biphasic $P_{\mathrm{tiss,O_2}}$ signal originates from increased oxygen consumption followed by increased oxygen supply due to the rise in CBF, and that this increase in oxygen supply is responsible for attenuating the negative $P_{\mathrm{tiss,O_2}}$ response.

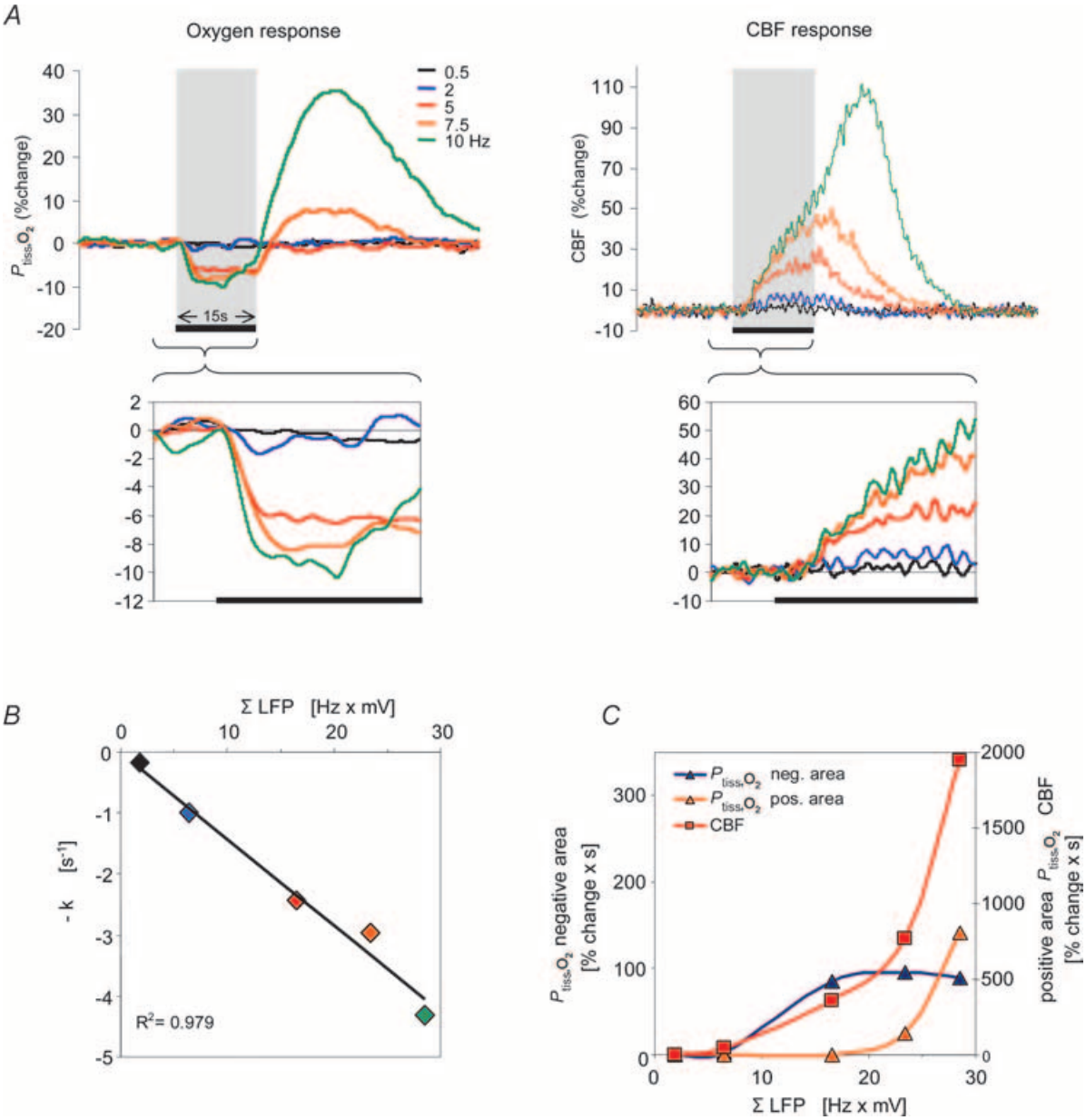


**Figure 2. Frequency-dependent changes of $P_{tiss,O_2}$, CBF and LFP responses: original recording from one animal**

A, superimposed $P_{tiss,O_2}$ and CBF responses (averages of four responses from one animal) to varying stimulation frequencies from 0.5 to 10 Hz. The $P_{tiss,O_2}$ response pattern ranged from monophasic decreases (0.5–5 Hz) to biphasic responses (7.5 and 10 Hz) where an initial decrease (negative $P_{tiss,O_2}$ response) was followed by a tissue oxygenation overshoot (positive $P_{tiss,O_2}$ response). The CBF response increased monotonically with increasing stimulation frequency. The inset boxes enlarge the responses during the stimulation period. The disappearance rate of oxygen in the tissue ($-k$) during the initial phase of stimulation, was frequency dependent (left inset), as indicated by the increasing steepness of the initial negative slope. Tissue deoxygenation began before CBF started to rise. The grey bars, and the black lines at the bottom of the inset boxes indicate the 15-s stimulation period. *B*, shows a correlation plot between ΣLFP during stimulation (averaged LFP amplitude × stimulation frequency) and $-k$. Colour coding is the same as in *A*. *C*, shows correlation plots between ΣLFP and evoked CBF, negative and positive $P_{tiss,O_2}$ responses.

### Effect of attenuated CBF rise on $P_{tiss,O_2}$ responses and synaptic activity

To validate the above hypothesis, we tried to clamp CBF during activation using 7-NI (40 mg kg$^{-1}$), which is a relatively selective, irreversible nNOS inhibitor. 7-NI effectively attenuates stimulation-induced CBF responses (Cholet *et al.* 1996; Yang *et al.* 1999; Lindauer *et al.* 1999), without affecting either resting or stimulation-induced cerebral glucose utilization (Cholet *et al.* 1997). Furthermore, NOS inhibition has no effect on stimulation-induced neuronal activity (Akgoren *et al.* 1996; Lindauer *et al.* 1996) or on the basal $CMRO_2$ (Iadecola *et al.* 1994; Chi *et al.* 2003). Thus 7-NI is a suitable pharmacological tool to investigate the effect of neuronal activation on tissue oxygenation changes under conditions of an attenuated CBF response.

In the present study, 7-NI did not result in significant changes of arterial blood gas parameters, MABP ($+1.6 \pm 1.6\%$) baseline CBF ($-11.4 \pm 6.3\%$), or baseline $P_{tiss,O_2}$ ($-0.8 \pm 2.7\%$). In the following experiments, 10 Hz stimulations were given repeatedly under control conditions and in the presence of 7-NI ($n = 8$). This stimulation frequency of 10 Hz was chosen as it was found to produce robust biphasic $P_{tiss,O_2}$ responses. Figure 5*A* shows an example of $P_{tiss,O_2}$ and CBF responses before (CTR) and after administration of 7-NI. 7-NI attenuated the stimulation-induced CBF increase by $60.3 \pm 4.6\%$ ($P = 0.003$; Fig. 5*B*). At the same time, the negative $P_{tiss,O_2}$ response increased fourfold ($+403.4 \pm 22.1\%$; $P = 0.01$), while the positive $P_{tiss,O_2}$ response decreased by $78.1 \pm 8.8\%$ ($P = 0.003$; Fig. 5*B*). These findings confirmed our hypothesis, which predicted that 7-NI would enlarge the negative and reduce the positive $P_{tiss,O_2}$ responses.

Interestingly, $-k$ was not affected by 7-NI ($+2.7 \pm 6.9\%$; $P = 0.71$). This indicated that the initial slope of the negative $P_{tiss,O_2}$ response was independent of the associated CBF rise (Fig. 6*C*). In comparison, both the positive and the negative $P_{tiss,O_2}$ areas depended on the magnitude of the evoked CBF response. The positive $P_{tiss,O_2}$ response was linearly correlated to the evoked CBF increase (Fig. 6*A*; linear regression analysis: $y = 0.673x - 37.2$; $R^2 = 0.67$, $P = 0.0001$) which demonstrated that the positive $P_{tiss,O_2}$ response in the cerebellum is indeed a consequence of increased oxygen supply. However, CBF had to rise above a certain threshold before a positive $P_{tiss,O_2}$ response was evident. The negative $P_{tiss,O_2}$ response decayed exponentially with increasing CBF (Fig. 6*B*). Of most importance, ΣLFP

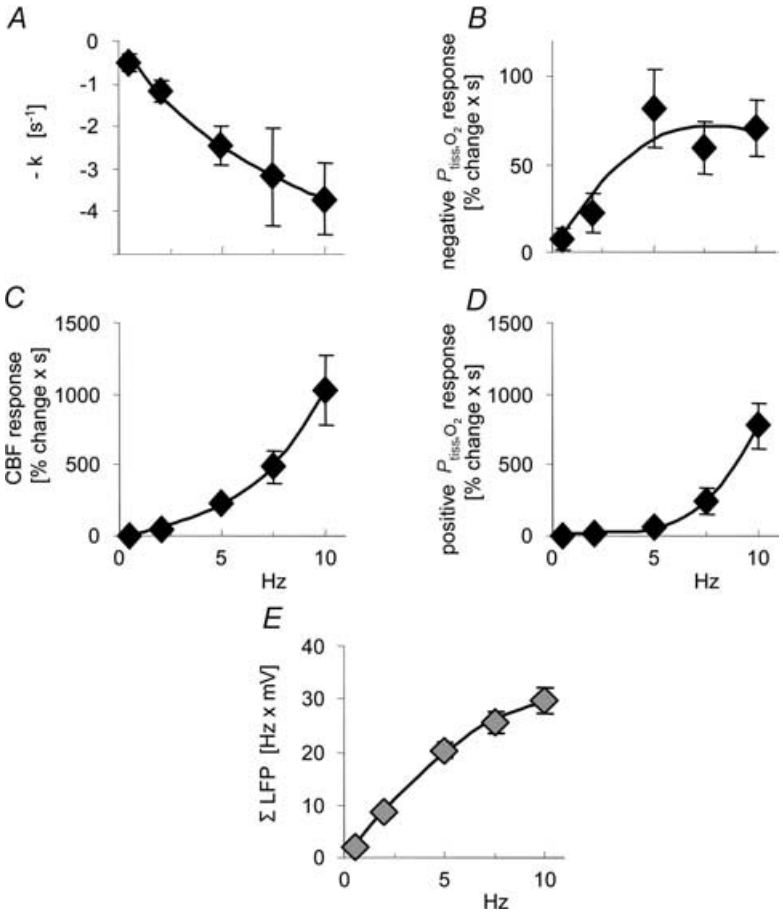


**Figure 3. Frequency-dependency of $P_{tiss,O_2}$ and CBF dynamics**
Stimulation-induced responses are plotted against stimulation frequencies ($n = 10$ rats). Data are averaged by frequency and illustrate the frequency dependency of the haemodynamic and oxygen responses. *A*, the disappearance rate of oxygen in the tissue ($-k$; initial slope of the negative $P_{tiss,O_2}$ response) increased with increasing stimulation frequency. *B*, a plot of the mean area of the negative $P_{tiss,O_2}$ response. The area of the negative $P_{tiss,O_2}$ response increased up to frequencies of 5 Hz and then levelled off. *C* and *D*, the CBF and positive $P_{tiss,O_2}$ responses showed an ongoing increase without signs of saturation. *E*, shows ΣLFP plotted against stimulation frequency. ΣLFP (expressing the overall level of synaptic activity) tends to saturate at frequencies above 5 Hz. The *x*-axis labels for *C* and *D* also apply for *A* and *B*. All values are given as mean ± S.E.M.

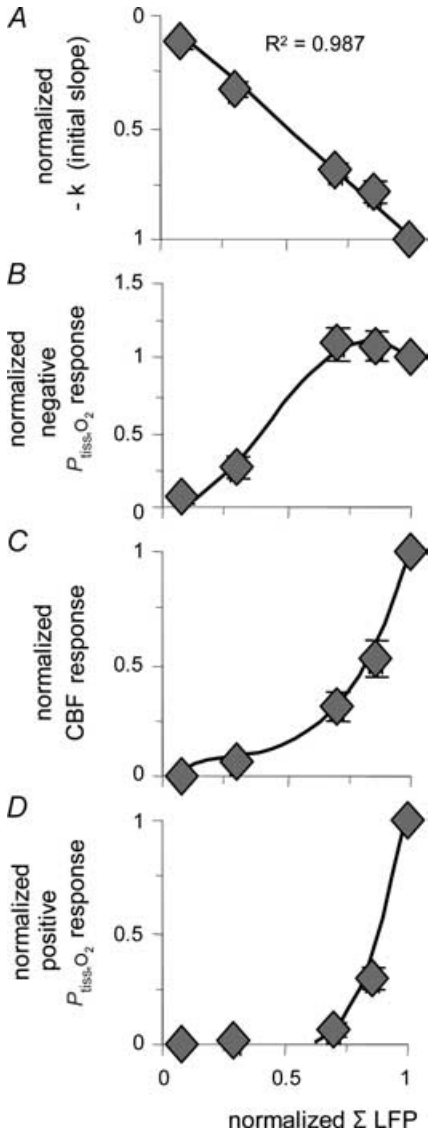


**Figure 4. Correlation between accumulated synaptic activity and $P_{tiss,O_2}$ and CBF responses**
Normalized values of evoked CBF and $P_{tiss,O_2}$ responses are plotted against normalized values of ΣLFP ($n = 10$ rats). All responses were normalized to the corresponding 10-Hz response and were averaged and grouped by stimulation frequency. *A*, the disappearance rate of oxygen in the tissue ($-k$) plotted against synaptic activity (ΣLFP) shows an inverse linear relationship, well fitted by a linear regression passing through the origin ($P < 0.05$). This suggests that oxygen consumption increases at all levels of synaptic activity. B, the correlation between ΣLFP and the area of the negative $P_{tiss,O_2}$ response demonstrated saturation of the negative $P_{tiss,O_2}$ response at high levels of synaptic activity. The CBF (*C*) and the positive $P_{tiss,O_2}$ response (*D*) both exhibited a non-linear rise over the range of induced synaptic activities without reaching saturation. *C* and *D*, indicate that synaptic activity, and thereby CBF, has to increase above a given threshold to evoke a $P_{tiss,O_2}$ overshoot. Note that the level of synaptic activity where the CBF response curve started to increase more steeply coincides not only with the point where a positive $P_{tiss,O_2}$ signal became evident but also with the point where the negative $P_{tiss,O_2}$ response started to level off. The *x*-axis label for *D* applies to all panels. Polynomial regression was used to illustrate the distribution of data in *B*–*D*. All values are given as mean ± S.E.M.

was not affected by NOS inhibition (−2.5%, $P = 0.26$; Fig. 5*C*). Thus, the observed changes in the $P_{tiss,O_2}$ signal were not due to reduced synaptic activity. So far, our findings indicated that the origin of the positive $P_{tiss,O_2}$ response is an increase in $O_2$ supply derived from the activation-induced increase in CBF. At the same time, the negative $P_{tiss,O_2}$ response is modulated by the increment in CBF.

### Effect of glutamate receptor blockade on synaptic transmission, $P_{tiss,O_2}$ and CBF responses

Here we examined whether postsynaptic activity in Purkinje cells could explain oxygen consumption during activation. Therefore, we studied the effect of AMPA receptor blockade on activation-induced $P_{tiss,O_2}$ changes. AMPA receptor blockade has previously been shown to effectively inhibit glutamate-mediated synaptic transmission at the climbing fibre–Purkinje cell synapse (Mathiesen *et al.* 1998). Beside this direct action of CNQX on postsynaptic excitation, indirect actions might increase inhibition (Brickley *et al.* 2001) or decrease disinhibition of Purkinje cells (Satake *et al.* 2000) which could also affect the Purkinje cell output (spiking) activity.

We found that superfusion of the cerebellum with the AMPA receptor antagonist, CNQX (0.5 mM), had no effect on MABP, baseline CBF (+2.8 ± 2.7%) or baseline $P_{tiss,O_2}$ (+2.2 ± 2.3%; $n = 8$). CNQX attenuated ΣLFP by 68.9 ± 7% ($P < 0.001$; Fig. 7*C*) and CBF responses by 69.0 ± 15.3% ($P < 0.001$; Fig. 7*A* and *B*; $n = 8$). At the same time, CNQX significantly inhibited both the negative (−81.3 ± 13.9%; $P = 0.004$) and the positive $P_{tiss,O_2}$ responses (−84.4 ± 8.1%, $P < 0.001$; Fig. 7*A* and *B*). All effects of CNQX were reversible with no significant differences between control conditions and washout (Fig. 7). These findings supported the idea that the decrease in tissue oxygenation seen during activation depends upon postsynaptic activity in Purkinje cells. This was confirmed by additional experiments in which CNQX was applied after pretreatment with 7-NI ($n = 5$; Fig. 8).

## Discussion

The direct assessment of local changes in $P_{tiss,O_2}$ in conjunction with CBF and electrophysiological recordings revealed a linear relationship between the disappearance rate of oxygen in the tissue and synaptic activity during the initial phase of neuronal activation in the cerebellar cortex. This increase in oxygen metabolism was evident at all levels of synaptic activity and depended on activation of glutamatergic AMPA receptors localized postsynaptically on Purkinje cell dendrites. Hence *in vivo*, early increases in neuronal aerobic metabolism depend on postsynaptic activity as previously shown *in vitro* for the hippocampus (Kasischke *et al.* 2004). During the initial phase of activation we observed a temporal uncoupling of oxidative

metabolism and CBF as a decline in $P_{tiss,O_2}$ was observed preceding the rise in CBF. Following the initial oxygen 'dip', $P_{tiss,O_2}$ increased due to the rise in CBF. Application of 7-NI attenuated the CBF rise, while increasing the negative $P_{tiss,O_2}$ response and decreasing the positive $P_{tiss,O_2}$ response. These findings imply that, in the cerebellum, the activity-induced reduction in $P_{tiss,O_2}$ is counteracted by an increase in oxygen supply due to the rise in CBF. The data also support the hypothesis that the positive $P_{tiss,O_2}$ response is an overshoot caused by the evoked increase in CBF. The fact that oxygen consumption increased before CBF suggests a reserve capacity of oxygen in the tissue as

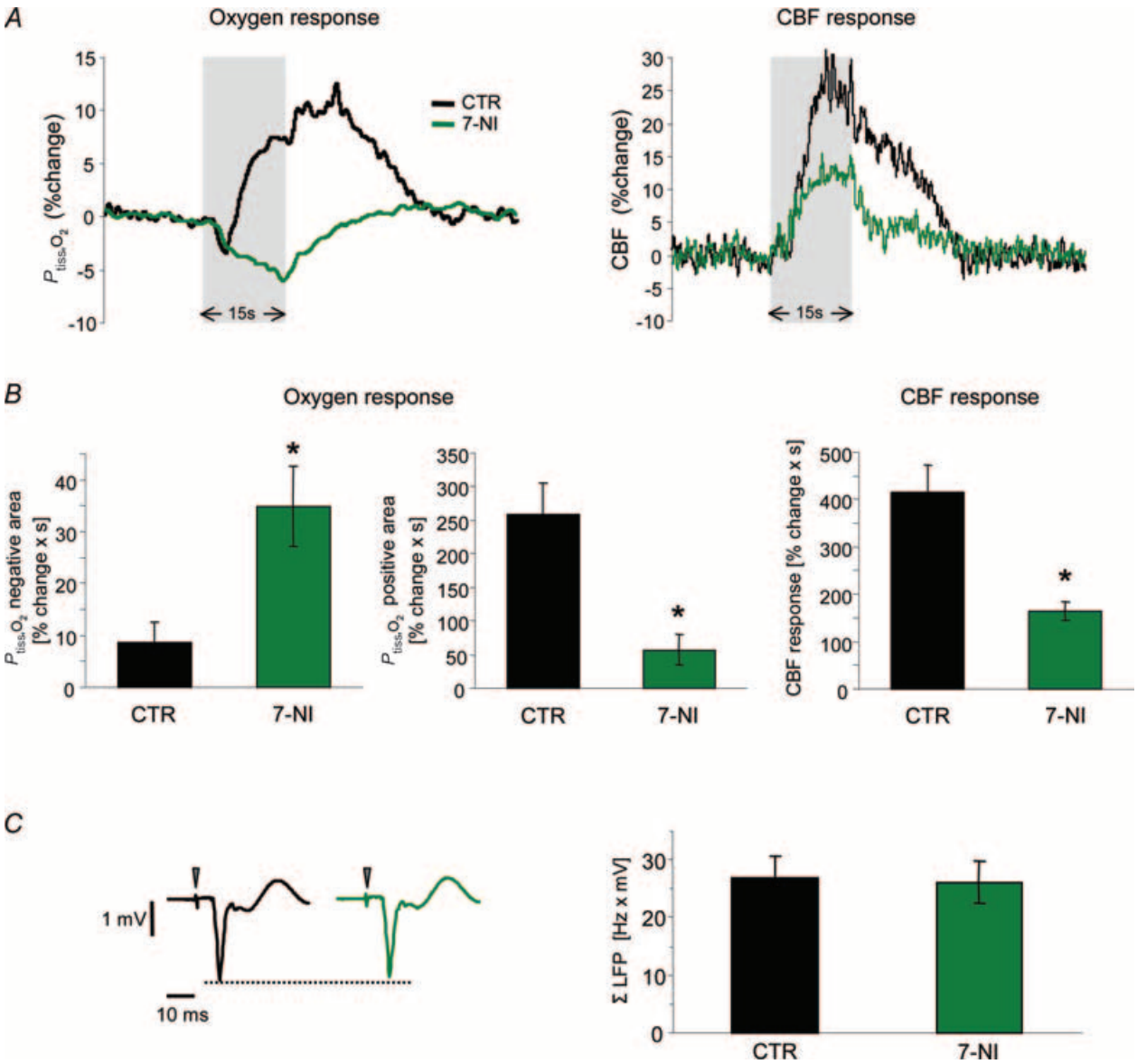


**Figure 5. Effect of attenuated CBF rise on $P_{tiss,O_2}$ responses and synaptic activity**
Responses to climbing fibre stimulation at 10 Hz were compared before (CTR) and after I.P. application of the nNOS inhibitor 7-nitroindazol (7-NI; $n = 8$ rats). *A*, shows an example of $P_{tiss,O_2}$ and corresponding CBF responses before (black) and after application of 7-NI (green). Grey bars denote the stimulation period. The biphasic $P_{tiss,O_2}$ response at this frequency was calculated as negative and positive $P_{tiss,O_2}$ response area. *B*, 7-NI enlarged the negative $P_{tiss,O_2}$ response by ~400% ($P < 0.05$) and reduced the positive $P_{tiss,O_2}$ response by ~78% ($P < 0.05$). These changes accompanied the attenuation of the evoked CBF rise of ~60% ($P < 0.05$) *B*, all values in *B* are given as mean ± S.E.M. *C*, demonstrates that the observed changes were not due to effects on synaptic activity, as ΣLFP was not significantly altered by 7-NI. *C,* left panel shows averaged LFPs before (black) and after (green) application of 7-NI from the same animal as in *A*. Time points of stimulation are marked by grey arrowheads. *$P < 0.05$.

proposed previously (Buxton, 2001; Mintun *et al.* 2001; Sheth *et al.* 2004).

### Negative $P_{tiss,O_2}$ and CBF response

In the present study, the typical $P_{tiss,O_2}$ response was biphasic with an initial decrease followed by an increase. The magnitude of both phases varied with the level of activity and differed between animals, reflecting the well-known spatial heterogeneity of $P_{tiss,O_2}$ profiles at rest and during activation (Gijsbers & Melzack, 1967; Silver, 1978; Lubbers *et al.* 1994; Erecinska & Silver, 2001; Masamoto *et al.* 2004). Despite this heterogeneity, initial $P_{tiss,O_2}$ reductions preceding evoked CBF responses were observed at all stimulation frequencies. This is consistent with previous studies in the somatosensory and visual cortices in which early decreases in tissue $P_{O_2}$ (Ances *et al.* 2001) or intravascular oxygen content (Malonek *et al.* 1997; Jones *et al.* 2001) occurred before significant CBF responses. The present study confirmed this response pattern in the cerebellar cortex. Our findings strengthen the concept that early activity-induced increases in deoxyhaemoglobin in optical imaging studies (Jones *et al.* 2001; Devor *et al.* 2003) and the initial dip seen in functional MRI (fMRI) studies (Menon *et al.* 1995; Kim *et al.* 2000) reflect local increases in oxygen consumption. The area of the negative $P_{tiss,O_2}$ response is thought to reflect changes in oxygen consumption and supply over time. The influence of activity-dependent increases in CBF for the $P_{tiss,O_2}$ response has been hypothesized previously (Silver, 1978; Ances *et al.* 2001; Masamoto *et al.* 2003*a*; Thompson *et al.* 2003) but has not been proven by simultaneous measurements of $P_{tiss,O_2}$, neuronal activity and CBF over a wide range of activities. For example Thompson *et al.* (2004) showed that activation of a small neuronal population induced a negative $P_{tiss,O_2}$ change that was partly cancelled out by a positive $P_{tiss,O_2}$ signal, which arose when a larger population of neurones was activated. They suggested that this was due to a rise in CBF, but CBF was not measured. We demonstrated by varying the synaptic input to a given population of neurones that the level of activity at which the negative $P_{tiss,O_2}$ area no longer increases coincided with the level of activity at which the CBF response curve escalated (Fig. 4*B* and *C*). The non-linear relationship found between evoked synaptic activity and CBF responses in the cerebellum was similar to those previously found in the cerebral cortex (Devor *et al.* 2003; Sheth *et al.* 2004).

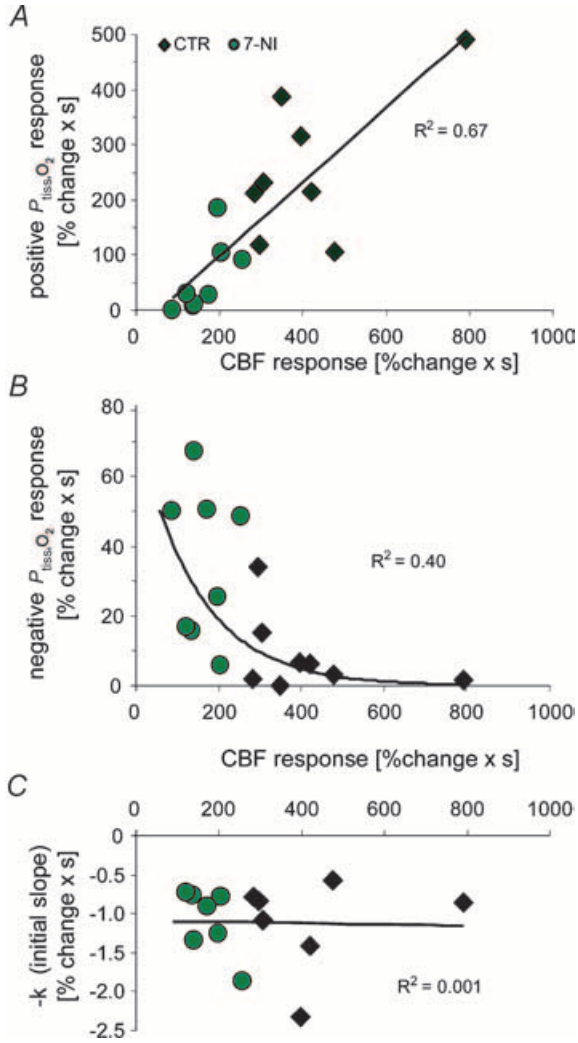


**Figure 6. Tissue $P_{O_2}$ responses in relation to CBF increases before and after application of 7-NI**
*A*, plotting the areas of positive $P_{tiss,O_2}$ responses to 10-Hz stimulations against corresponding CBF responses shows that small positive $P_{tiss,O_2}$ responses correspond to small increases in CBF obtained after 7-NI application (green circles), while large positive $P_{tiss,O_2}$ responses correspond to large increases in CBF obtained during control conditions (♦) ($n = 8$ rats). This indicates a linear relationship between positive $P_{tiss,O_2}$ signals and increases in CBF (linear regression analysis, $P < 0.05$). *B*, the areas of negative $P_{tiss,O_2}$ responses decayed exponentially with increasing magnitude of CBF responses ($y = 75.012e - 0.0069x$). *C*, in contrast to the positive and negative $P_{tiss,O_2}$ responses, the disappearance rate of oxygen in the tissue ($-k$) was independent of the magnitude of evoked CBF responses.

The hypothesis that the reduction of the negative $P_{tiss,O_2}$ area was caused by increased oxygen supply due to greatly increased CBF responses was further tested in the 7-NI experiments. We found that the negative $P_{tiss,O_2}$ area increased and the positive $P_{tiss,O_2}$ area decreased as the magnitude of the activity-evoked CBF responses declined in the presence of 7-NI. Thus, this study clearly demonstrated an inverse relationship between the negative $P_{tiss,O_2}$ area and the CBF response, and that at high levels of activation, the negative $P_{tiss,O_2}$ area, and thereby estimates of oxygen consumption based upon this parameter, are confounded by increased $O_2$ supply. We conclude that the non-linear relationship between the negative $P_{tiss,O_2}$ area and synaptic activity is explained by increased CBF and oxygen supply and not by a reduction in oxygen consumption.

### Tissue and intravascular deoxygenation during activation

The non-linearity between synaptic activity and negative $P_{tiss,O_2}$ area in the present study raises important issues concerning the initial dip observed with optical imaging techniques and fMRI and whether it can accurately reflect the magnitude of underlying neuronal activity (Nemoto *et al.* 2004). $P_{O_2}$ in the tissue lies between capillary and mitochondrial $P_{O_2}$ levels and shows a high susceptibility to changes in oxygen consumption (Secomb *et al.* 2000). The increased oxygen concentration gradient in the tissue during activation (Vanzetta & Grinvald, 1999; Ances *et al.* 2001; Thompson *et al.* 2003) results

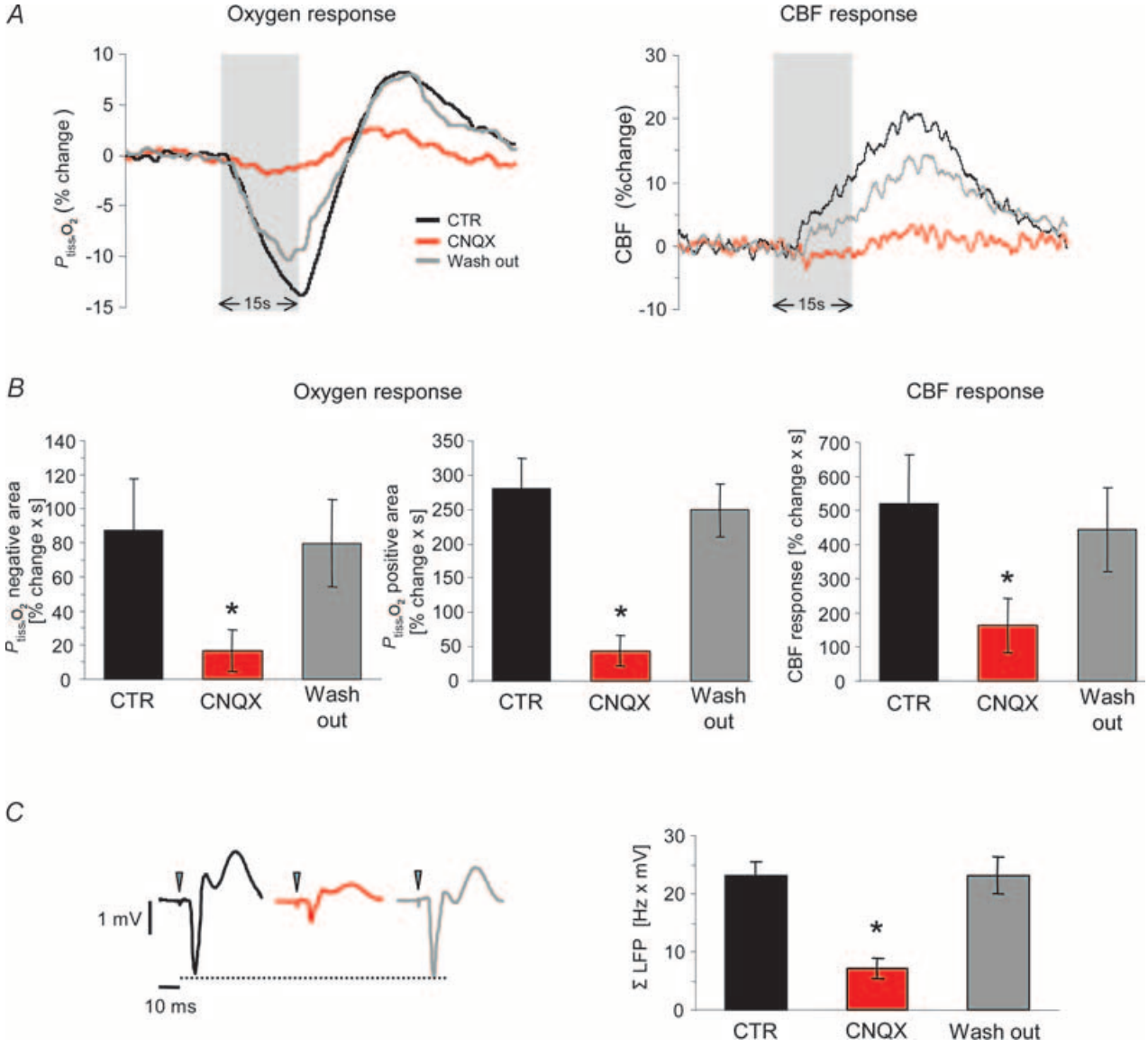


**Figure 7. Effect of AMPA receptor blockade on synaptic transmission, and evoked $P_{tiss,O_2}$ and CBF responses**

The effect of topically applied CNQX on responses evoked by climbing fibre stimulation at 10 Hz is illustrated ($n = 8$ rats). Responses obtained before (CTR), during (CNQX) and after wash out (Wash out) were compared. *A*, shows an example of $P_{tiss,O_2}$ and corresponding CBF responses before (black trace), during (red trace) and after washout of CNQX (grey trace). Grey bars denote the stimulation period. *B*, AMPA receptor blockade reversibly attenuated both phases of the $P_{tiss,O_2}$ response and the CBF increase (negative $P_{tiss,O_2}$ response area, −81%; positive $P_{tiss,O_2}$ response area, −84%; CBF response, −69%). All values in *B* are given as mean ± S.E.M. *C*, the concomitant inhibition of ΣLFP during AMPA receptor blockade (−69%, $P < 0.05$, right panel) indicated that the reduction of the $P_{tiss,O_2}$ responses in the presence of CNQX was due to reduced postsynaptic activity. *C*, left panel shows averaged LFPs before (black), during (red) and after wash out (grey) of CNQX from the same animal as in *A*. Time points of stimulation are marked by grey arrowheads. *$P < 0.05$ compared to CTR.

in increased conversion of oxy- to deoxyhaemoglobin. Hence, deoxygenation signals from tissue and vasculature are linked in their response to neuronal activation. We found that the magnitude of the negative $P_{tiss,O_2}$ area, representing tissue deoxygenation, reaches a plateau at high levels of neuronal activity (Fig. 4*B*). Thus, the initial dip representing intravascular deoxygenation cannot be expected to increase at high levels of neuronal activity when tissue deoxygenation does not. This implies that the initial dip calculated as peak response or area might not be capable of indicating increases in neuronal activity beyond a given threshold, which could explain some of the inconsistent findings in optical imaging studies correlating neuronal activity to the magnitude of the initial dip (Mayhew *et al.* 2000; Devor *et al.* 2003; Sheth *et al.* 2003, 2004; Nemoto *et al.* 2004).

### Initial slope and activity-dependent increases in early oxygen consumption

As the relationship between synaptic activity and the area of the negative $P_{tiss,O_2}$ response was confounded by CBF, we then assessed the initial slope of the negative $P_{tiss,O_2}$ response ($-k$) to obtain a relative measure of activity-induced oxygen consumption. Local oxygen consumption has previously been determined in absolute terms in the brain cortex and hippocampus by using $O_2$-disappearance measurements during brief periods of total brain ischaemia (Leniger-Follert, 1977; Buerk & Nair, 1993). In the present study, $-k$ was independent of the associated CBF rises, implying that $-k$ is a reliable indicator of early increases in oxygen consumption during activation in the cerebellum. Unlike the negative $P_{tiss,O_2}$ response area, $-k$ did increase as a linear function

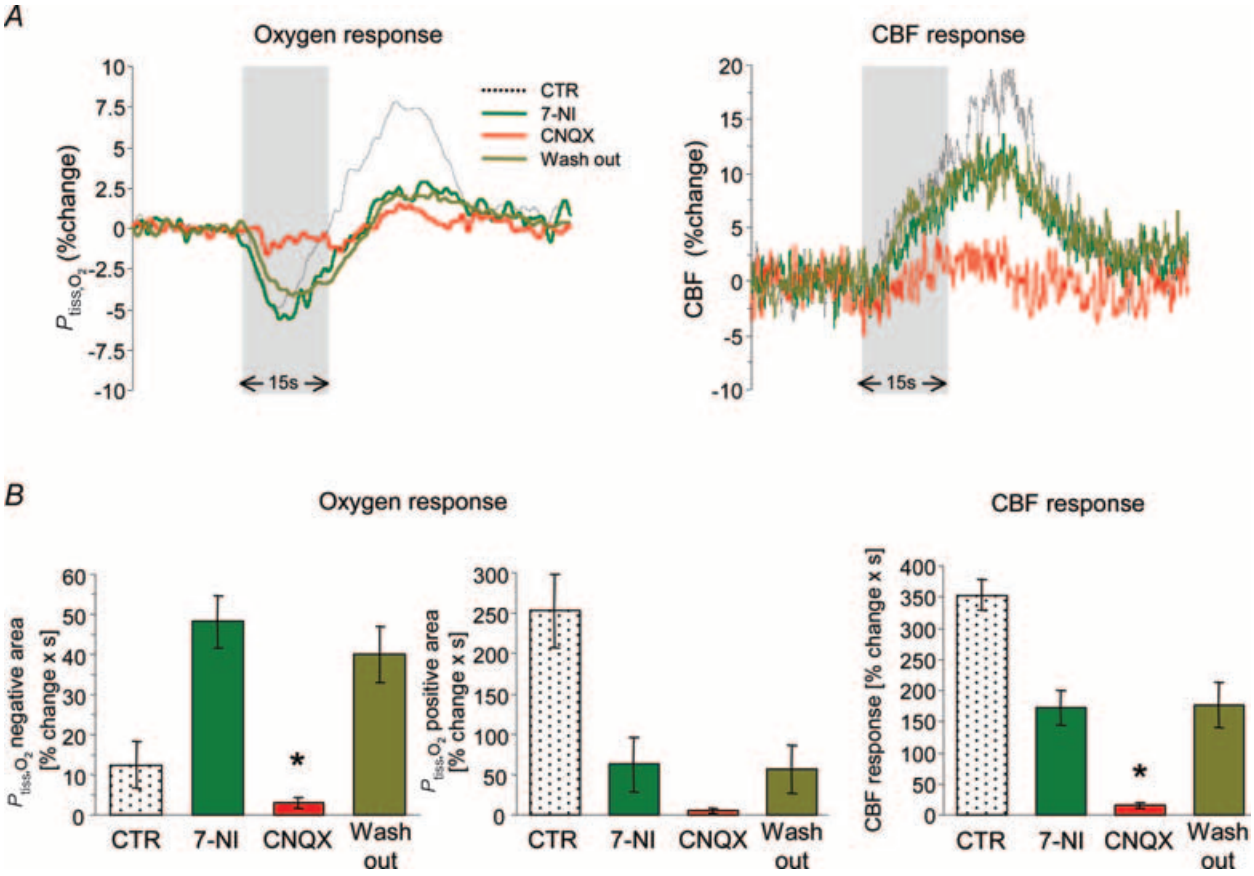


**Figure 8. Effect of AMPA receptor blockade after pretreatment with 7-NI**
CNQX (0.5 mM) was topically applied in five out of eight animals treated with 7-NI and responses evoked by climbing fibre stimulation at 10 Hz were compared. *A*, shows an example of $P_{tiss,O_2}$ and corresponding CBF responses from one animal under control conditions (black trace), after application of 7-NI (dark green), in the presence of 7-NI + CNQX (red) and after washout of CNQX (bright green). Grey bars denote the stimulation period. *B*, shows the averaged responses before (CTR) and after application of 7-NI (7-NI) and illustrates the temporary effect of CNQX (CNQX and Wash out). As 7-NI is an irreversible nNOS inhibitor, it cannot be washed out. Compared to 7-NI values, the negative $P_{tiss,O_2}$ response during application of CNQX was reduced by ~94%. The already diminished positive $P_{tiss,O_2}$ and CBF responses were both further reduced by ~91%. However, the decrease in the positive $P_{tiss,O_2}$ response did not reach significance. CNQX application attenuated the ΣLFP by 85% (compared to 7-NI; $P < 0.05$; data not shown). All CNQX effects were reversible with no significant differences to 7-NI. All values are given as mean ± S.E.M. $^*P < 0.05$ compared to 7-NI.

of synaptic activity (i.e. ΣLFP; Fig. 4*A*). This confirms previous findings using optical imaging techniques, which calculated that peak $CMRO_2$ increased with growing stimulation intensities (Jones *et al.* 2001) and that the relationship between ΣLFP and increases in $CMRO_2$ was linear (Sheth *et al.* 2004). Sheth *et al.* (2004) calculated that increased oxygen extraction from the vasculature occurs only above a given threshold of synaptic activity. In comparison, we found no such threshold in the cerebellum, indicating that tissue oxygen consumption increased at even the lowest levels of synaptic activity. This, in conjunction with the observed non-linear increase of CBF with synaptic activity, supports the idea that at rest a significant amount of readily available oxygen in the tissue exists which might serve as a tissue oxygen reserve (Buxton, 2001; Mintun *et al.* 2001). Importantly, the present study indicated that an increase in local oxygen consumption occurs in response to activation and that this increase is linearly related to the level of synaptic activity.

Using the initial slope ($-k$) to represent oxygen consumption during activation, we found that the relationship between evoked oxygen consumption and CBF responses was non-linear (Fig. 4*A* and *C*). Our data are at variance with other studies reporting a 2 : 1 linear relationship between CBF and $CMRO_2$ changes (Hoge *et al.* 1999; Sheth *et al.* 2004), but are consistent with mathematical models of tissue oxygen delivery predicting a supra-linear relationship (Buxton & Frank, 1997; Hudetz, 1999; Vafaee & Gjedde, 2000; Secomb *et al.* 2000).

### Neurometabolic coupling

Activity-induced changes in $P_{\mathrm{tiss,O_2}}$ have been explored in a number of studies (Travis & Clark, 1965; Gijsbers & Melzack, 1967; Sick & Kreisman, 1979; Ances *et al.* 2001) but recently the relationship between neuronal activity and oxygen consumption has been assessed more directly by recording the two variables simultaneously in the same location. This has shown that negative $P_{\mathrm{tiss,O_2}}$ changes are highly specific for local increases in neuronal activity and quantitatively related to the amount of underlying neuronal activity (Thompson *et al.* 2003; Masamoto *et al.* 2003*a*), although the type of neuronal activity has not been established. Masamoto *et al.* (2003*a*) related neuronal activity induced by single activation tasks to voltage-sensitive dye recordings which, however, allowed no discrimination between pre- and postsynaptic activation. Thompson *et al.* (2003, 2004) focused on the local specificity of tissue deoxygenation signals in relation to spike recordings and confirmed a correlation between spiking activity and negative tissue $P_{O_2}$ responses during activation (Sick & Kreisman, 1979). As neurotransmission and synaptic input in most neuronal circuits are prerequisites for spike generation and are often linearly correlated to changes in output spiking activity (Devor *et al.* 2003; Jones *et al.* 2004), it is not possible to deduce by spike measurements alone whether glutamate release, postsynaptic processing or output firing is responsible for the increased oxygen demand during activation.

During climbing fibre stimulation, we observed a linear relationship between synaptic activity and $-k$ as discussed above. Topical application of CNQX almost abolished synaptic transmission as well as the evoked negative $P_{\mathrm{tiss,O_2}}$ response, identifying postsynaptic AMPA receptor activation as necessary for early negative $P_{\mathrm{tiss,O_2}}$ changes. Astrocytes are not activated during electrical stimulation of Purkinje cell afferents as reported in an immunohistochemical study (Tian & Bishop, 2002). Thus, in the climbing fibre–Purkinje cell pathway, increases in oxygen consumption are coupled to activity in postsynaptic neurones. As the climbing fibre–Purkinje cell synapse is one of the most powerful excitatory synapses where glutamatergic transmission leads to activation of AMPA receptors on one of the widest dendritic trees, it has to be determined whether oxygen consumption in other brain regions is also mainly driven by postsynaptic activation. Our findings are consistent with a nuclear magnetic resonance spectroscopy study by Sibson *et al.* (1998), who showed that rates of neuronal CMRO2 and glutamate release and cycling are stoichiometrically related. However, our study cannot be used to differentiate between oxygen used for postsynaptic processing and oxygen used for generation of spikes. We conclude that the observed early increase in oxygen consumption during activation *in vivo* is of neuronal origin as has been previously shown in the hippocampus *in vitro* (Kasischke *et al.* 2004). Furthermore, the results of the present study demonstrate that neuronal oxygen consumption in the cerebellar cortex increases together with synaptic activity.

### Neuronal activity and oxygen transport to tissue

There is still debate concerning the coupling between blood flow responses and oxygen consumption during activation in the brain. Oxygen-limitation models designed to explain this coupling have been based on the assumption that at rest all oxygen in the tissue is consumed and $P_{O_2}$ at the level of the mitochondria is zero (Buxton & Frank, 1997; Hyder *et al.* 1998; Vafaee & Gjedde, 2000). However during activation, we observed that oxygen consumption in the tissue increased before CBF did, and that in the presence of 7-NI, the magnitude of the negative $P_{\mathrm{tiss,O_2}}$ area increased despite the strong attenuation of the CBF response. These observations suggest that resting $P_{\mathrm{tiss,O_2}}$ is far from zero. Our findings support the existence of a tissue oxygen reserve and are in line with human positron emission tomography data (Mintun *et al.* 2001), calculations of resting tissue oxygenation levels in the brain (Secomb *et al.* 2000) and recent modelling of tissue oxygen delivery (Hudetz, 1999; Mintun *et al.* 2001). The results

from our study imply that in the anaesthetized state, the cerebellum has an excess oxygen delivery at rest and that this tissue oxygen reserve is used during the initial phase and at low grades of activation. We suggest that up to a given level of neuronal activity, oxygen consumption can increase even under conditions of constant CBF. On the other hand, the finding of a supra-linear relationship between CBF and $CMRO_2$ changes during activation provides experimental confirmation of the predictions derived from the oxygen-limitation models (Buxton & Frank, 1997; Vafaee & Gjedde, 2000). According to these models, oxygen diffusivity is limited (Gjedde *et al.* 1991) and during activation, increases in oxygen consumption are supported by disproportionately large increases in CBF (Buxton & Frank, 1997). Combined, our data support the recently proposed hypothesis that a buffer of oxygen availability in the tissue exists and that CBF increases during activation are regulated to maintain this buffer (Buxton, 2001).

### Conclusion

In this study we examined the physiological basis of activity-induced changes in tissue oxygen tension in rat cerebellar cortex. We showed that $P_{\mathrm{tiss,O_2}}$ responses are the result of a temporally staggered interplay between neuronal oxygen consumption and evoked CBF increments both driven by postsynaptic activity. At the level of the climbing fibre–Purkinje cell synapse, tissue oxygen consumption is linearly coupled to synaptic excitation with no evidence of a threshold; thus, we found that tissue energy demands are supplied by oxidative metabolism at all levels of synaptic activity. We have also quantitatively assessed the relationships between synaptic activity and tissue oxygenation signals and CBF responses. The findings indicate a supralinear relationship between increases in oxygen consumption and CBF during activation and support the existence of a buffer of oxygen availability in brain tissue.

## References


Akgoren N, Dalgaard P & Lauritzen M (1996). Cerebral blood flow increases evoked by electrical stimulation of rat cerebellar cortex: relation to excitatory synaptic activity and nitric oxide synthesis. *Brain Res* **710**, 204–214.

Ances BM, Buerk DG, Greenberg JH & Detre JA (2001). Temporal dynamics of the partial pressure of brain tissue oxygen during functional forepaw stimulation in rats. *Neurosci Lett* **306**, 106–110.

Attwell D & Laughlin SB (2001). An energy budget for signaling in the grey matter of the brain. *J Cereb Blood Flow Metab* **21**, 1133–1145.

Baumgartl H, Zimelka W & Lubbers DW (2002). Evaluation of $PO_2$ profiles to describe the oxygen pressure field within the tissue. *Comp Biochem Physiol A Mol Integr Physiol* **132**, 75–85.

Beitz AJ & Saxon D (2004). Harmaline-induced climbing fiber activation causes amino acid and peptide release in the rodent cerebellar cortex and a unique temporal pattern of Fos expression in the olivo-cerebellar pathway. *J Neurocytol* **33**, 49–74.

Brickley SG, Farrant M, Swanson GT & Cull-Candy SG (2001). CNQX increases GABA-mediated synaptic transmission in the cerebellum by an AMPA/kainate receptor-independent mechanism. *Neuropharmacology* **41**, 730–736.

Buerk DG & Nair P (1993). $PtiO_2$ and $CMRO_2$ changes in cortex and hippocampus of aging gerbil brain. *J Appl Physiol* **74**, 1723–1728.

Buxton RB (2001). The elusive initial dip. *Neuroimage* **13**, 953–958.

Buxton RB & Frank LR (1997). A model for the coupling between cerebral blood flow and oxygen metabolism during neural stimulation. *J Cereb Blood Flow Metab* **17**, 64–72.

Chi OZ, Liu X & Weiss HR (2003). Effects of inhibition of neuronal nitric oxide synthase on NMDA-induced changes in cerebral blood flow and oxygen consumption. *Exp Brain Res* **148**, 256–260.

Cholet N, Bonvento G & Seylaz J (1996). Effect of neuronal NO synthase inhibition on the cerebral vasodilatory response to somatosensory stimulation. *Brain Res* **708**, 197–200.

Cholet N, Seylaz J, Lacombe P & Bonvento G (1997). Local uncoupling of the cerebrovascular and metabolic responses to somatosensory stimulation after neuronal nitric oxide synthase inhibition. *J Cereb Blood Flow Metab* **17**, 1191–1201.

Clarke DD & Sokoloff L (1994). Circulation and energy metabolism of the brain. In *Basic Neurochemistry: Molecular, Cellular, and Medical*, ed. Siegel GJ, Agranoff BW, Albers RW & Molinoff PB, pp. 645–680. Raven Press, New York.

Devor A, Dunn AK, Andermann ML, Ulbert I, Boas DA & Dale AM (2003). Coupling of total hemoglobin concentration, oxygenation, and neural activity in rat somatosensory cortex. *Neuron* **39**, 353–359.

Dunbar RL, Chen G, Gao W, Reinert KC, Feddersen R & Ebner TJ (2004). Imaging parallel fiber and climbing fiber responses and their short-term interactions in the mouse cerebellar cortex in vivo. *Neuroscience* **126**, 213–227.

Eccles JC, Ito M & Szentágothai J (1967). *The Cerebellum as a Neuronal Machine*. Springer, New York.

Eccles JC, Llinas R & Sasaki K (1966). The excitatory synaptic action of climbing fibres on the purkinje cells of the cerebellum. *J Physiol* **182**, 268–296.

Erecinska M & Silver IA (2001). Tissue oxygen tension and brain sensitivity to hypoxia. *Respir Physiol* **128**, 263–276.

Foster KA & Regehr WG (2004). Variance-mean analysis in the presence of a rapid antagonist indicates vesicle depletion underlies depression at the climbing fiber synapse. *Neuron* **43**, 119–131.

Fukuda M, Yamamoto T & Llinas R (2001). The isochronic band hypothesis and climbing fibre regulation of motricity: an experimental study. *Eur J Neurosci* **13**, 315–326.

Gijsbers KJ & Melzack R (1967). Oxygen tension changes evoked in the brain by visual stimulation. *Science* **156**, 1392–1393.

Gjedde A, Ohta S, Kuwabara H & Meyer E (1991). Is oxygen diffusion limiting for blood-brain transfer of oxygen? In *Brain Work and Mental Activity*, ed. Lassen NA, Ingvar DH, Raichle ME & Friberg L, pp. 177–184. Munksgaard, Copenhagen.

Hanson CL, Chen G & Ebner TJ (2000). Role of climbing fibers in determining the spatial patterns of activation in the cerebellar cortex to peripheral stimulation: an optical imaging study. *Neuroscience* **96**, 317–331.

Harrison J & Jahr CE (2003). Receptor occupancy limits synaptic depression at climbing fiber synapses. *J Neurosci*, **23**, 377–383.

Hoge RD, Atkinson J, Gill B, Crelier GR, Marrett S & Pike GB (1999). Linear coupling between cerebral blood flow and oxygen consumption in activated human cortex. *Proc Natl Acad Sci U S A* **96**, 9403–9408.

Hudetz AG (1999). Mathematical model of oxygen transport in the cerebral cortex. *Brain Res* **817**, 75–83.

Hyder F, Shulman RG & Rothman DL (1998). A model for the regulation of cerebral oxygen delivery. *J Appl Physiol* **85**, 554–564.

Iadecola C (2004). Neurovascular regulation in the normal brain and in Alzheimer's disease. *Nat Rev Neurosci* **5**, 347–360.

Iadecola C, Pelligrino DA, Moskowitz MA & Lassen NA (1994). Nitric oxide synthase inhibition and cerebrovascular regulation. *J Cereb Blood Flow Metab* **14**, 175–192.

Jones M, Berwick J, Johnston D & Mayhew J (2001). Concurrent optical imaging spectroscopy and laser-Doppler flowmetry: the relationship between blood flow, oxygenation, and volume in rodent barrel cortex. *Neuroimage* **13**, 1002–1015.

Jones M, Hewson-Stoate N, Martindale J, Redgrave P & Mayhew J (2004). Nonlinear coupling of neural activity and CBF in rodent barrel cortex. *Neuroimage* **22**, 956–965.

Kasischke KA, Vishwasrao HD, Fisher PJ, Zipfel WR & Webb WW (2004). Neural activity triggers neuronal oxidative metabolism followed by astrocytic glycolysis. *Science* **305**, 99–103.

Kim DS, Duong TQ & Kim SG (2000). High-resolution mapping of iso-orientation columns by fMRI. *Nat Neurosci* **3**, 164–169.

Konnerth A, Llano I & Armstrong CM (1990). Synaptic currents in cerebellar Purkinje cells. *Proc Natl Acad Sci U S A* **87**, 2662–2665.

Lauritzen M (2005). Opinion: Reading vascular changes in brain imaging: is dendritic calcium the key? *Nat Rev Neurosci* **6**, 77–85.

Leniger-Follert E (1977). Direct determination of local oxygen consumption of the brain cortex in vivo. *Pflugers Arch* **372**, 175–179.

Lennie P (2003). The cost of cortical computation. *Curr Biol* **13**, 493–497.

Lindauer U, Megow D, Matsuda H & Dirnagl U (1999). Nitric oxide: a modulator, but not a mediator, of neurovascular coupling in rat somatosensory cortex. *Am J Physiol* **277**, H799–H811.

Lindauer U, Megow D, Schultze J, Weber JR & Dirnagl U (1996). Nitric oxide synthase inhibition does not affect somatosensory evoked potentials in the rat. *Neurosci Lett* **216**, 207–210.

Llano I, Marty A, Armstrong CM & Konnerth A (1991). Synaptic- and agonist-induced excitatory currents of Purkinje cells in rat cerebellar slices. *J Physiol* **434**, 183–213.

Llinas R, Leznik E & Makarenko VI (2002). On the amazing olivocerebellar system. *Ann N Y Acad Sci* **978**, 258–272.

Llinas R & Nicholson C (1974). Analysis of field potentials in the central nervous system. In *Handbook of Electroencephalography and Clinical Neurophysiology*, Vol. 2, Part B ed. Remond A, pp. 61–85. Elsevier Scientific Publishing Co, Amsterdam.

Llinas R & Volkind RA (1973). The olivo-cerebellar system: functional properties as revealed by harmaline-induced tremor. *Exp Brain Res* **18**, 69–87.

Lubbers DW, Baumgartl H & Zimelka W (1994). Heterogeneity and stability of local $PO_2$ distribution within the brain tissue. *Adv Exp Med* **345**, 567–574.

Malonek D, Dirnagl U, Lindauer U, Yamada K, Kanno I & Grinvald A (1997). Vascular imprints of neuronal activity: relationships between the dynamics of cortical blood flow, oxygenation, and volume changes following sensory stimulation. *Proc Natl Acad Sci U S A* **94**, 14826–14831.

Masamoto K, Kurachi T, Takizawa N, Kobayashi H & Tanishita K (2004). Successive depth variations in microvascular distribution of rat somatosensory cortex. *Brain Res* **995**, 66–75.

Masamoto K, Omura T, Takizawa N, Kobayashi H, Katura T, Maki A, Kawaguchi H & Tanishita K (2003*a*). Biphasic changes in tissue partial pressure of oxygen closely related to localized neural activity in guinea pig auditory cortex. *J Cereb Blood Flow Metab* **23**, 1075–1084.

Masamoto K, Takizawa N, Kobayashi H, Oka K & Tanishita K (2003*b*). Dual responses of tissue partial pressure of oxygen after functional stimulation in rat somatosensory cortex. *Brain Res* **979**, 104–113.

Mathiesen C, Caesar K, Akgoren N & Lauritzen M (1998). Modification of activity-dependent increases of cerebral blood flow by excitatory synaptic activity and spikes in rat cerebellar cortex. *J Physiol* **512**, 555–566.

Mayhew J, Johnston D, Berwick J, Jones M, Coffey P & Zheng Y (2000). Spectroscopic analysis of neural activity in brain: increased oxygen consumption following activation of barrel cortex. *Neuroimage* **12**, 664–675.

Menon RS, Ogawa S, Hu X, Strupp JP, Anderson P & Ugurbil K (1995). BOLD based functional MRI at 4 Tesla includes a capillary bed contribution: echo-planar imaging correlates with previous optical imaging using intrinsic signals. *Magn Reson Med* **33**, 453–459.

Mintun MA, Lundstrom BN, Snyder AZ, Vlassenko AG, Shulman GL & Raichle ME (2001). Blood flow and oxygen delivery to human brain during functional activity: theoretical modeling and experimental data. *Proc Natl Acad Sci U S A* **98**, 6859–6864.

Nemoto M, Sheth S, Guiou M, Pouratian N, Chen JW & Toga AW (2004). Functional signal- and paradigm-dependent linear relationships between synaptic activity and hemodynamic responses in rat somatosensory cortex. *J Neurosci* **24**, 3850–3861.

Nicholson C & Llinas R (1971). Field potentials in the alligator cerebellum and theory of their relationship to Purkinje cell dendritic spikes. *J Neurophysiol* **34**, 509–531.

Nielsen A & Lauritzen M (2001). Coupling and uncoupling of activity-dependent increases of neuronal activity and blood flow in rat somatosensory cortex. *J Physiol* **533**, 773–785.

Obata T, Liu TT, Miller KL, Luh WM, Wong EC, Frank LR & Buxton RB (2004). Discrepancies between BOLD and flow dynamics in primary and supplementary motor areas: application of the balloon model to the interpretation of BOLD transients. *Neuroimage* **21**, 144–153.

Raichle ME (1998). Behind the scenes of functional brain imaging: a historical and physiological perspective. *Proc Natl Acad Sci U S A* **95**, 765–772.

Raichle ME (2003). Functional brain imaging and human brain function. *J Neurosci* **23**, 3959–3962.

Revsbech NP (1989). An oxygen microsensor with a guard cathode. *Limnol Oceanogr* **34**, 474–478.

Satake S, Saitow F, Yamada J & Konishi S (2000). Synaptic activation of AMPA receptors inhibits GABA release from cerebellar interneurons. *Nat Neurosci* **3**, 551–558.

Secomb TW, Hsu R, Beamer NB & Coull BM (2000). Theoretical simulation of oxygen transport to brain by networks of microvessels: effects of oxygen supply and demand on tissue hypoxia. *Microcirculation* **7**, 237–247.

Sheth S, Nemoto M, Guiou M, Walker M, Pouratian N & Toga AW (2003). Evaluation of coupling between optical intrinsic signals and neuronal activity in rat somatosensory cortex. *Neuroimage* **19**, 884–894.

Sheth SA, Nemoto M, Guiou M, Walker M, Pouratian N & Toga AW (2004). Linear and nonlinear relationships between neuronal activity, oxygen metabolism, and hemodynamic responses. *Neuron* **42**, 347–355.

Sibson NR, Dhankhar A, Mason GF, Rothman DL, Behar KL & Shulman RG (1998). Stoichiometric coupling of brain glucose metabolism and glutamatergic neuronal activity. *Proc Natl Acad Sci U S A* **95**, 316–321.

Sick TJ & Kreisman NR (1979). Local tissue oxygen tension as an index of changes in oxidative metabolism in the bullfrog optic tectum. *Brain Res* **169**, 575–579.

Siesjo BK (1978). *Brain Energy Metabolism*. Wiley, New York.

Silver IA (1978). Cellular microenvironment in relation to local blood flow. In *Cerebral Vascular Smooth Muscle and its Control*, *CIBA Foundation Symposium* **56**, pp. 49–67. Elsevier, Excerpta-Medica, North Holland.

Silver RA, Momiyama A & Cull-Candy SG (1998). Locus of frequency-dependent depression identified with multiple-probability fluctuation analysis at rat climbing fibre-Purkinje cell synapses. *J Physiol* **510**, 881–902.

Thompson JK, Peterson MR & Freeman RD (2003). Single-neuron activity and tissue oxygenation in the cerebral cortex. *Science* **299**, 1070–1072.

Thompson JK, Peterson MR & Freeman RD (2004). High-resolution neurometabolic coupling revealed by focal activation of visual neurons. *Nat Neurosci* **7**, 919–920.

Thomsen K, Offenhauser N & Lauritzen M (2004). Principle neuron spiking: neither necessary nor sufficient for cerebral blood flow in rat cerebellum. *J Physiol* **560**, 181–189.

Tian JB & Bishop GA (2002). Stimulus-dependent activation of c-Fos in neurons and glia in the rat cerebellum. *J Chem Neuroanat* **23**, 157–170.

Travis RP Jr & Clark LC Jr (1965). Changes in evoked brain oxygen during sensory stimulation and conditioning. *Electroencephalogr Clin Neurophysiol* **19**, 484–491.

Vafaee MS & Gjedde A (2000). Model of blood-brain transfer of oxygen explains nonlinear flow-metabolism coupling during stimulation of visual cortex. *J Cereb Blood Flow Metab* **20**, 747–754.

Vanzetta I & Grinvald A (1999). Increased cortical oxidative metabolism due to sensory stimulation: implications for functional brain imaging. *Science* **286**, 1555–1558.

Yang G, Chen G, Ebner TJ & Iadecola C (1999). Nitric oxide is the predominant mediator of cerebellar hyperemia during somatosensory activation in rats. *Am J Physiol* **277**, R1760–R1770.

## Acknowledgements

We thank Lillian Grondahl for expert technical assistance, and Jesper Grondahl for his sophisticated MatLab programming. This study was supported by The Lundbeck Foundation, the Danish Medical Research Council, Vera and Carl Michelsens legat, and The NOVO-Nordisk Foundation.